

Book of Tutorials and Abstracts



European Microbeam Analysis Society

EMAS 2019

**16th
EUROPEAN WORKSHOP**

on

**MODERN DEVELOPMENTS
AND
APPLICATIONS
IN
MICROBEAM ANALYSIS**

19 to 23 May 2019
at the
NTNU, Realfagbygget
Trondheim, Norway

Organised in collaboration with:
Norwegian University of Science and Technology
(NTNU)



SPATIAL RESOLUTION LIMITS OF EPMA

Ben Buse and S.L. Kearns

University of Bristol, School of Earth Sciences
Wills Memorial bldg., Queen's Road, Bristol BS8 1RJ, Great Britain
e-mail: ben.buse@bristol.ac.uk

After a degree in Geology and Physical Geography at the University of Bristol, Ben Buse completed a PhD at the University of Bristol looking at the metamorphism of kimberlites (the rocks that contain diamonds!) in Botswana. Subsequent work has concentrated on electron microprobe analysis with postdoctoral positions at the Microbeam Labs at the University of Bristol and briefly at the Nanyang Technological University, Singapore. Ben has for the last seven years worked at the microbeam labs at the University of Bristol, with Stuart Kearns. He has 14 scientific publications the majority of which cover analysis of geological materials.

1. ABSTRACT

The development of field emission EPMA, has significantly improved the lateral resolution of EPMA. Two strategies are available for achieving high spatial resolution, either low overvoltage or low voltage analysis. Determining the spatial resolution for a particular analysis is complex and depends on the voltage, spot size, beam current, density of the sample, X-rays analysed and the precision and sensitivity required. At low overvoltage or low voltage conditions many additional factors must be considered: carbon contamination, coat thickness, erosion of the carbon coat, the stability of the sample and the problems surrounding the measurement of soft X-ray lines including L-lines for first row transition metals. By taking these factors into consideration, high quality measurements can be made.

2. INTRODUCTION

Electron probe microanalysis (EPMA) has traditionally employed a thermionic tungsten source analysing material on the scale of several cubic micrometres (for densities of 2 - 5 g/cm²), at accelerating voltages of 15 - 20 kV. Field emission gun (FEG) EPMA, which employs a sharpened tungsten crystal to reduce the source area of electron emission and provides a dense beam of electrons, and permits higher spatial resolution to be achieved at low voltage [1]. High spatial resolution is important for analysing small phases or inclusions, diffusion profiles and particles, although geometry must be considered for the latter. Monte Carlo simulation is often used to image the scattering and deceleration of the electron beam on entering a material. At high accelerating voltages (15 - 20 kV) the electron range (the distance electrons travel into the sample) is several microns (Fig. 1) whilst the beam diameter (spot size) is comparatively small (10s - 100s nm) even for a conventional tungsten source. At low accelerating voltages (< 10 kV) the electron range is 100s nm (Fig. 1), making the spot size (10s - 100s nm) an important component of the lateral resolution (Fig. 2), exacerbated by the increase in beam diameter at lower accelerating voltages [1].

There has been excellent work by Pinard and Richter [3] and McSwiggen [4] characterising the interaction volume for a focussed beam as the accelerating voltage is reduced for FEG-EPMA at a constant beam current. The interaction volume initially reduces and then increases reflecting the interplay of electron range and spot size, with reduced accelerating voltage resulting in the electron range decreasing whilst spot size is increasing. Minimum interaction volumes were found to be typically in the 5 - 8 kV range. This may be calculated using Monte Carlo simulations for a range of beam currents, if the change in spot size with beam current and accelerating voltage is known, allowing the detection limit and precision to be considered and therefore the ability for trace elements to be measured at a given spatial resolution.

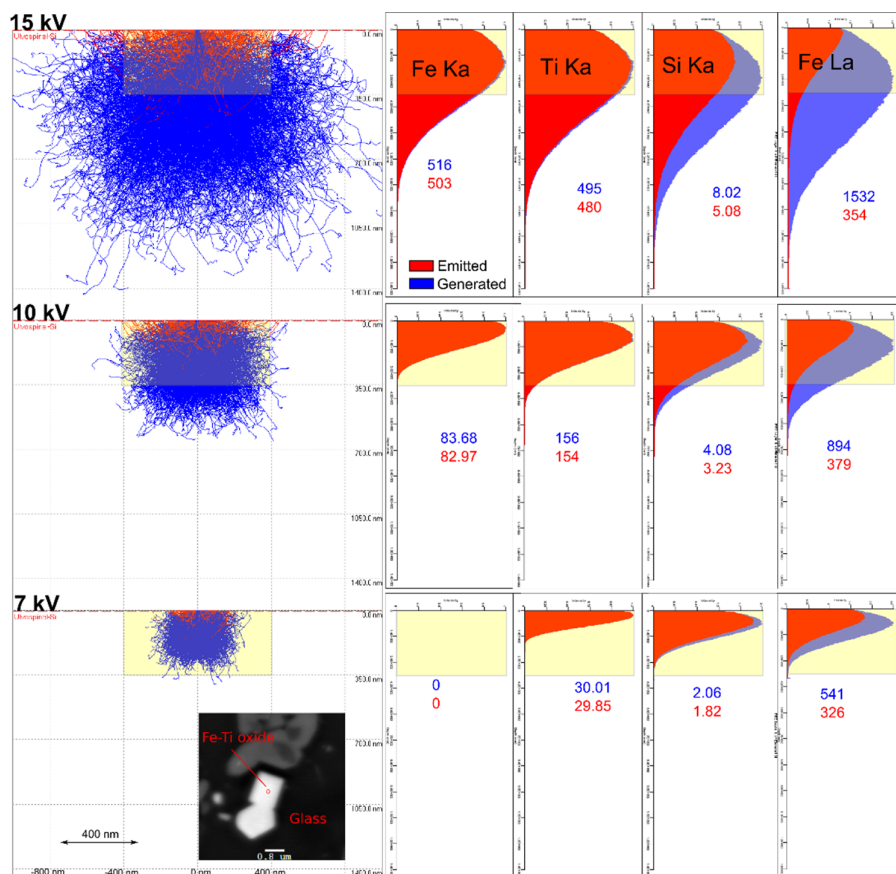


Figure 1. Monte Carlo simulations (using Casino [2]) for bulk ulvospinel (Fe_2TiO_4) with trace Si and a density of 4.78 g/cm^3 for a beam diameter of 10 nm. On the left is the electron distribution, with backscattered electrons coloured red; on the right are the phi-rho-z curves for different elements. The yellow box represents the size of a $800 \times 350 \text{ nm}$ crystal, a typical size of minerals formed during high pressure experiments; see BSE image insert. Table 1 gives analyses for this crystal.

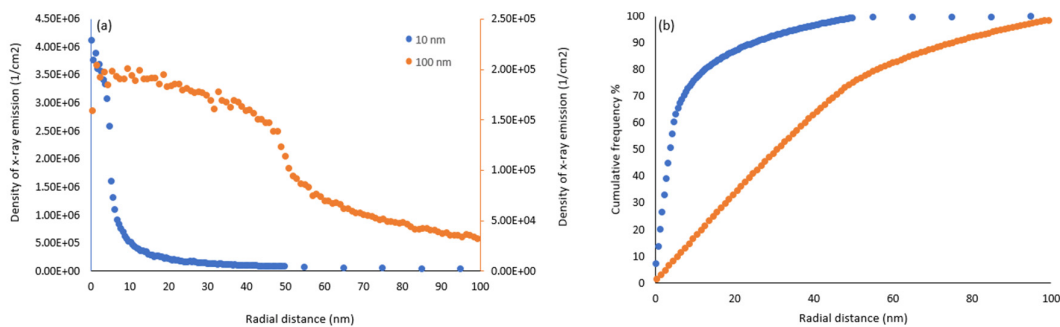


Figure 2. Fe-L α radial distribution of X-rays calculated using PENEPMA Monte Carlo simulation [5] for ulvospinel at 7 kV.

Pinard and Richter [3] and McSwiggen [4] instead of considering the electron range and electron interaction volume, consider the volume from which X-rays are emitted. This determines the spatial resolution of chemical analysis and is termed ‘analytical volume’ by McSwiggen [3]. Given that different X-rays have different critical excitation energies at a single accelerating voltage, different X-rays will have different analytical volumes. If the overvoltage (the ratio of accelerating voltage to X-ray critical excitation energy) is small, X-rays are generated close to the point at which the electron beam enters the sample (e.g., Fe K α at 10 kV, Fig. 3). The low overvoltage means that only a small loss of energy is required before the beam is unable to excite the X-ray of interest. Whereas if the overvoltage is large the analytical volume will closely correspond to the electron interaction volume (e.g., Si K α at 10 kV, Fig. 3). The depth of the analytical volume is also dependent on the amount of absorption of the X-ray by the sample, determined by the mass absorption coefficient (MAC); in the case of oxygen K α or Fe L α which are soft X-rays (< 1 keV) and have high MACs only those X-rays generated near the surface are emitted and detected (e.g., Fe L α at 20 kV, Fig. 3). This however has little effect on the lateral width of the analytical volume.

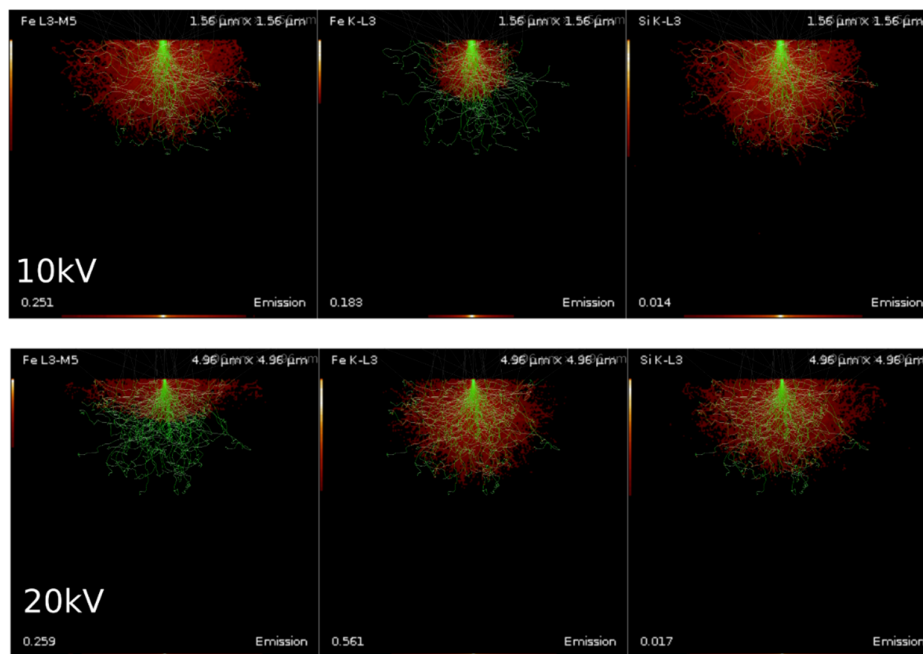


Figure 3. Integrated 2D X-Z slices displaying the source of emitted X-rays generated from Monte Carlo simulations using DTSA2 [6]. Red dots represent sites at which emitted X-rays are generated, green lines trace the electron trajectories.

3. STRATEGIES FOR OBTAINING HIGH SPATIAL RESOLUTION

Two strategies are available for obtaining high spatial resolution in bulk samples (e.g., [3, 4, 7]; see [8] for very thin samples), either a low voltage resulting in a small electron interaction

volume or a low overvoltage, which may be at high accelerating voltage for a high energy X-ray, resulting in a small analytical volume for the X-ray of interest. Using low accelerating voltages allows multiple X-rays to be measured at a single accelerating voltage, with spatial resolution equal to or less than that of the interaction volume. In the example of the 350 nm thick Ulvospinel in Fig. 1, all the elements could be analysed at 7 kV. Low voltage, however, limits the X-rays that can be excited (e.g., Fe L rather than Fe K at 7 kV), often restricting the analyst to soft X-rays which may be problematic. Problems include the close spacing of X-rays with the potential for peak overlaps, X-ray peaks may be subject to shifts and peak shape changes for different compounds (e.g., K-lines of B,N,C and O [9]) or axial orientation (e.g., B K α [9]) and in the cases of L α X-rays of first row transition metals and M α X-rays of rare earth elements anomalous self absorption occurs (e.g., [10-12]). Surface layers also become significant, reducing the beam energy entering the sample and absorbing soft X-rays. The following must be considered: (1) thickness of conductive coat [13], including erosion of a carbon coat by the electron beam, where high current density is used (small beam size and high beam current) particularly at low accelerating voltages [14]; (2) presence of oxide layers on metal samples [15]; and (3) carbon contamination, commonly deposited in a ring around the electron beam (see Fig. 4) affecting closely spaced analyses [16, 17].

Analysis at low overvoltage conditions at high voltages, avoids the necessity to use soft X-rays but low overvoltage conditions will only be satisfied for a few elements at a single voltage requiring multiple voltage analysis. In the example of the 350 nm Ulvospinel of Fig. 1, Fe K α can be analysed at 10 kV, whilst Ti and Si must be analysed at 7 kV, to keep the analytical volume within the ulvospinel (see Table 1 for results). At low overvoltages surface layers (contamination, conductive coats, and oxide layers) become very significant (see Fig. 4, also [14, 17]), with a small reduction in beam energy entering the sample resulting in a large drop in X-rays generated.

Table 1. Quantification of a 800 nm wide ulvospinel in a Si-rich, Fe-poor glass at multiple voltages, using the K α X-ray line for Fe. To achieve a reasonable quantification, Fe must be analysed at 10 kV, whilst the other elements analysed at 7 kV (see Fig. 1).

	MgO	SiO2	CaO	FeO	Na2O	Al2O3	K2O	TiO2	Total
15kV	1.24	26.37	0.71	59.15	1.13	6.47	0.72	11.39	107.15
10kV	1.29	4.73	0.18	76.48	0.04	1.64	0.09	15.47	99.90
7kV	1.32	1.36	0.24	76.479 (10kV)	0.01	0.98	0.05	17.52	97.96

Methods to mitigate the problems of surface layers include reducing carbon contamination by using liquid nitrogen or Peltier-cooled cold fingers (e.g., [17-19]), empirical correction [17], oxygen air jets for samples without a conductive carbon coat [18] and sample preparation by focussed ion beam (FIB) milling or cross-section polishing by Ar-ions to remove surface contaminations [20]. Recently for metal samples, Yamashita et al. [21] demonstrated the

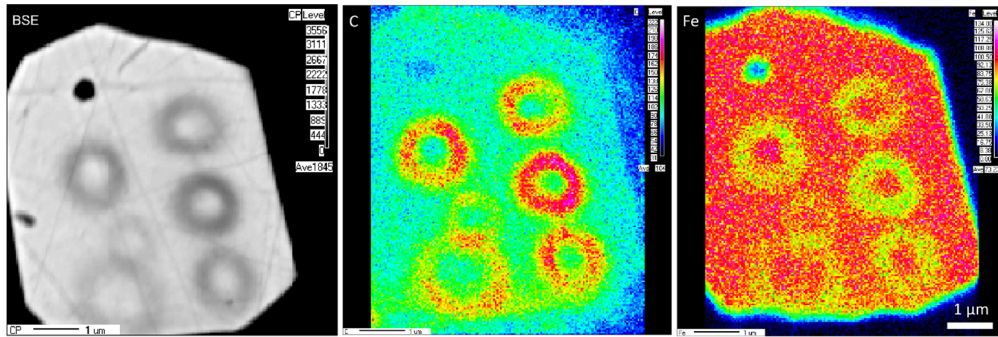


Figure 4. Backscatter electron (BSE) image and C and Fe X-ray intensity maps of analysis spots on a Fe-Ti spinel. Carbon contamination forms rings around the point of electron beam impact. At low overvoltage (accelerating voltage: 8.5 kV, critical excitation energy of Fe-K α : 7.1) carbon contamination strongly reduces Fe K α intensity.

effectiveness of in chamber plasma cleaning, sample heating together with a liquid nitrogen cold trap. Problems of the electron beam erosion of the carbon coat can be mitigated by: (1) reducing the current density, which may compromise either resolution or precision, (2) switching to a different conductive coat material, or (3) correcting for X-ray intensity change using time-dependent-correction (TDI) [14].

4. FIRST ROW TRANSITION METAL L-LINE ANALYSIS

For the analysis of many materials, first row transition metals are important. For low voltage analysis it may not be possible to excite the K-line X-rays, requiring analysis of the L-line X-rays. There has been considerable research exploring the complications in quantifying these lines. In 1985, Pouchou and Pichoir [22] demonstrated for Ni alloys, that the L α X-rays suffered from anomalous self-absorption and partial fluorescence yields, with absorption varying not just with element concentration but the structure of the valance band which is affected by the chemical environment (chemical bonding of atoms) requiring different MACs for different compositions. Similarly, the partial fluorescence yield varies with composition. Pouchou and Pouchoir [22] showed that for a binary series the MAC and partial fluorescence yield can be calculated using regression, allowing quantification. Fialin [23] noted the problem in MACs changing with electronic structure for Zn minerals and therefore standards and unknowns may have different MACs. More recently, Llovet *et al.* [24] applied this approach to Ni silicides, and Buse and Kearns [25] to olivines and showed that if solid-solution MACs and partial fluorescence yields are incorporated in matrix corrections quantification is possible, to an accuracy of $\leq 4\%$ relative. In examining olivines, Buse and Kearns [25] illustrated some of the difficulties in this approach; it requires measuring off-peak for some compositions and measuring the MAC across the absorption edge, where it is highly sensitive to the position of measurement. Moy and Fournelle [26] have instead of using conventional WDS peak and background measurements, have derived peak intensities through spectra deconvolution, from which MACs and partial fluorescence yields have been derived.

Remond *et al.* [27] tried a different approach to deal with anomalous absorption of $L\alpha$ and $L\beta$, by acquiring spectra, from which absorption spectra were calculated and used to correct the spectra. Using this method, they successfully analysed Fe_2O_3 with a FeO standard.

Other approaches to the analysis of first row transition metals have been tried. Gopon *et al.* [28] analysed Fe silicides using the Fe- $L\ell$ noting that unlike the Fe- $L\alpha$ and $-L\beta$ X-ray lines it was not affected by bonding. This method has yielded improved quantification compared to using the Fe $L\alpha$ -line without correcting for bonding effects. Statham & Holland [7] tested the $L\ell$ -line for measurement of steels, again finding improved quantification compared to $L\alpha$, although Cr- $L\ell$ was 9 % relative below the expected value. The $L\ell$ typically has low intensity compared to the $L\alpha$ -, $L\beta$ -lines limiting sensitivity and precision [7, 28]. Another solution is the use of calibration curves, allowing the use of the higher intensity $L\alpha$ - and $L\beta$ -lines whilst avoiding a knowledge of the variation in MACs and fluorescence yields, such as demonstrated by Buse and Kearns [29] for olivine.

5. ACHIEVING HIGH SPATIAL RESOLUTION FOR FE-BEARING MINERALS

Fe-bearing minerals demonstrate the problems in analysing first row transition metals at high resolution. In this section, we analysis Fe-bearing minerals using the two strategies outlined above. To address the problems of L-line analysis several approaches are used: (1) Fe- $L\ell$ analysis, (2) calibration curve for Fe- $L\alpha$ analysis when re-peaking on each sample, and (3) calibration curve for Fe- $L\alpha$ analysis with a fixed position. In addition comparisons are made to the results of Buse and Kearns [25] which calculated solid-solution MACs and partial fluorescence corrections for olivine analysis using Fe- $L\alpha$. Measurements were made on a JEOL 8530F FEG EPMA at the University of Bristol. A Peltier cold finger [19] was used during analysis to minimise contamination.

5.1. Fe- $K\alpha$ low overvoltage measurements

Analysing the Fe $K\alpha$ -line with an accelerating voltage of 10 kV, gives an overvoltage of 1.4 and yields low ionisation with net counts ca. 100 cps/nA on Fe metal using LIF compared to 1,200 – 1,600 cps/nA at 20 kV for the same crystals. Comparable precision therefore requires longer count times and/or higher beam currents. High precision was obtained for the measurements e.g., 0.8 % rel. (2σ) for St John's Island Olivine with 7.5 wt% Fe, using a high beam current (100 nA) and long count times (60 seconds on peak) and two spectrometers combined. The results are shown in Fig. 5, comparing measured values to reference values. The results are accurate to within 5 % relative and generally insensitive to the choice of standard.

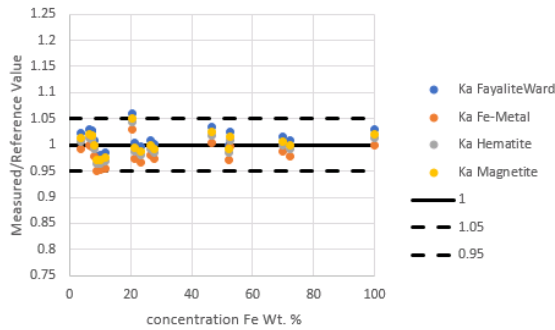


Figure 5. Fe-K α measurements at 10 kV compared to reference values, using 4 different materials as a standard.

5.2. Fe-L ℓ measurements

The Fe L ℓ -line was measured at 7 kV, 200 nA for 120 seconds on peak using a TAPH crystal. Careful background selection is required to avoid interference with Fe-L η and Mn-L α peaks; in this case only the upper background measurement was used. Fe-L ℓ has low net intensities of 4.37 cps/nA on Fe metal. This is primarily a function of the refracting crystal, for despite the low fluorescence yield of L3 shell vacancies, this is compensated by the large number of ionisations. L3 shell vacancies are either filled by electrons from the M5 shell to yield L α X-rays, or the M1 shell to yield L ℓ X-rays. L α X-rays dominate, although the relative intensity depends on the occupancy of the 3d electron shell, which varies with element [30, 31] and bonding.

The low intensities are reflected in the larger errors at the low concentrations (Fig. 6a). The accuracy of the results varies considerably between samples, with some samples differing from reference values by > 5 % relative. The calculated concentrations are sensitive to the standard used (Fig. 6b), with magnetite standard giving the best results for the dataset, whilst Fe metal performing poorly. A look at the peak positions for fayalite and Fe metal shows that this poor performance is not due to peak shift or shape.

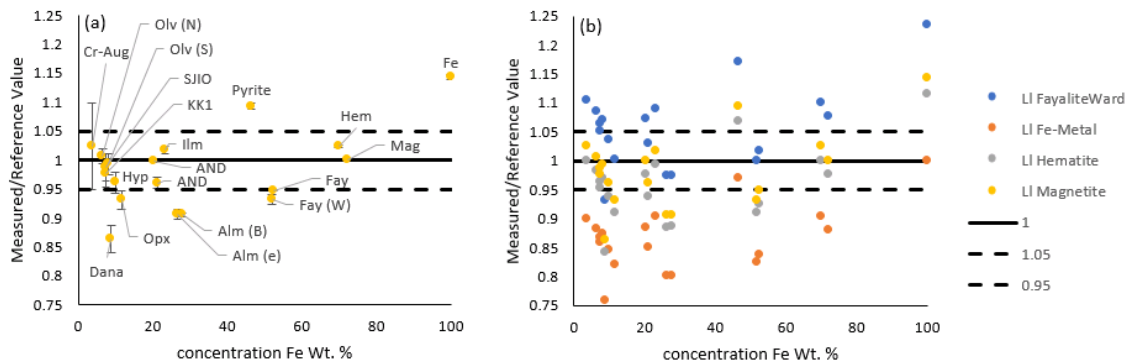


Figure 6. Fe-L ℓ measurements at 7 kV compared to reference values using a) magnetite, and b) 4 different materials as the standard. 1 sigma error bars shown for (a).

5.3. Fe-La measurements

Fe La was measured at 7 kV, 200 nA, on a TAP crystal, counting for 60 seconds on peak. Two methods of measuring the Fe La-line were tested, one using a fixed peak position (that of Fe metal), the other peaking up on each sample. To understand the changes in peak position, Fig. 7 shows the shift in peak positions (see [32]). The La-peak position shifts to high wavelengths with increasing Fe content as the low wavelength side is strongly absorbed by the Fe L3 absorption edge. As Hofer and Brey [33] for garnets and Fialin *et al.* [32] for a range of minerals have shown Fe self-absorption is greatest for Fe²⁺, with Fe³⁺ resulting in a shift in the absorption edge away from the La peak maximum. Therefore, as Fialin *et al.* [32] showed, on Fig. 7 the samples with Fe³⁺ have peak positions at lower wavelengths consistent with less self-absorption.

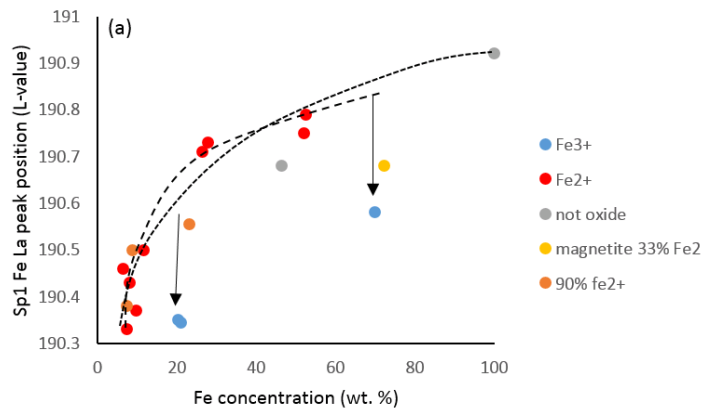


Figure 7. Fe La-peak, colour coded in terms of their Fe oxidation state. There is uncertainty where to plot the trend line, and whether it is continuous with Fe metal.

Figures 8 and 9 give the results for La using a fixed position and re-peaking on each sample. To interpret the results we must consider the measurement position relative to the peak maximum, the true emission peak position (the peak maximum without self-absorption), and the position of absorption maximum. In Fig. 8 each measurement is at peak maximum, but the peak maximum moves away from the true emission peak (and the absorption maximum) as absorption erodes the low wavelength side of the peak. In Fig. 9 the measurements are at the Fe metal peak, which is easy to accurately define, and reflects the emission peak for Fe metal. However, whilst this is close to the peak maximum for the minerals with high Fe content (see Fig. 7) as a result of absorption resulting in peak shift, it is a long way from the true emission peak, approximated by the low Fe content samples which have suffered less absorption (see Fig. 7, also [25, 32]). Both datasets show a tendency for calculated *k*-ratios to overestimate, particularly at high concentrations where self-absorption is higher. This corresponds to elevated MACs for minerals containing oxygen compared to Fe metal, consistent with the findings of Buse and Kearns [25] and Moy and Fournelle [34] for olivine. The opposite is seen for pyrite, where the calculated *k*-ratio underestimates, this is consistent with pyrite having a lower MAC than Fe metal, similar to that observed by Llovet *et al.* [24] for Ni-silicides.

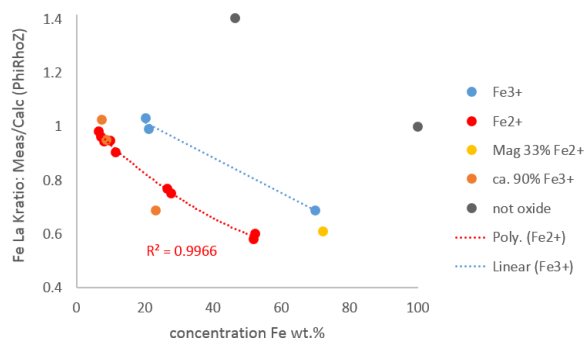


Figure 8. Fe-La measurements, on peak maximum, with peak search for each sample. Colour coded for Fe chemical state.

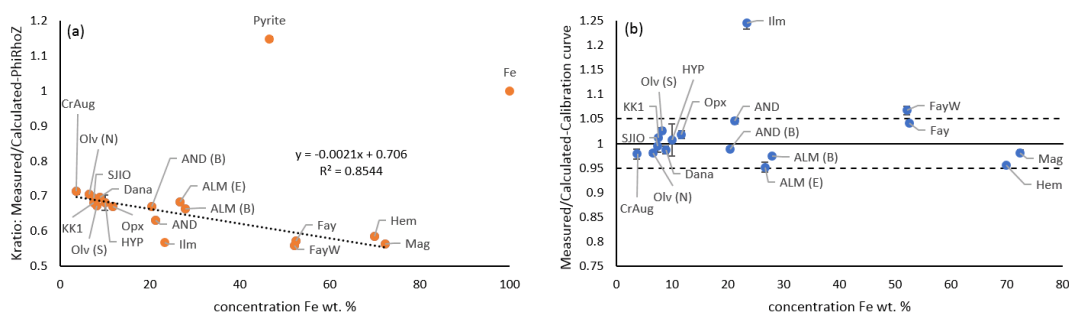


Figure 9. Fe-La measurements using a fixed peak position. a) Measured k -ratios compared to calculated k -ratios using Phi-Rho-Z models. Regression does not include pyrite and Fe metal; b) Measured k -ratios compared to calculated k -ratios using a calibration curve, here pyrite and Fe are off-scale. 1 sigma error bars are plotted.

If we compare the two sets of measurements, it can be seen that by re-peaking on each sample, the discrepancy between measured and calculated k -ratios is largely removed for minerals with low Fe-content, where measurement is now close to the true emission peak and absorption is minimal. At high Fe contents, re-peaking has little effect as the peak maxima are close to Fe metal. Crucially whilst measurement using peak maximum differentiates between Fe^{2+} and Fe^{3+} minerals and is, therefore, sensitive to the differences in self-absorption with Fe valence state; measurement using a fixed peak position is not sensitive to this. This appears to result from the elevated Fe-La intensities for Fe^{3+} minerals (in response to suffering less self-absorption), compensated by their offset peak position relative to Fe metal, which is also a consequence of the lower self-absorption.

6. DISCUSSION

The measurements made for Fe using the $\text{K}\alpha$ X-ray at low overvoltage and L-line X-rays at low voltage provide us with a good position for examining the various options for high spatial resolution and their merits. The Fe- $\text{K}\alpha$ gave the most reliable results both accurate and precise for all the materials measured including both pyrite and Fe metal and was insensitive to the

standard used. The limitation being that whilst the spatial resolution for Fe-K α at 10 kV is very good (depth < 350 nm for ulvospinel, Fig. 1) to achieve a similar resolution for the other elements such as Si (or more usefully Mg, Al) and Ti in the case of ulvospinel measurement at several voltages is required (as given in Table 1). Carbon contamination has not affected the results, for the analyses were widely spaced and a cold-finger was used; problems would arise if a very small spacing were required, such that the analysis point overlapped the carbon contamination of the previous point. Even using a cold-finger errors of a few percent relative can be introduced [17]. The measurements were made at 10 μ m avoiding the possibility of eroding the carbon coat. To achieve high lateral resolution a small spot size is required. At 10 kV, 100 nA beam current, a spot size of 100 nm can be achieved [3]. This degrades the lateral resolution by ca. 100 nm (see figure 2) making it significantly worse than the depth resolution. Poorer lateral resolution is acceptable for polished cubic phases where the depth is typically substantially less than the width. At small spot sizes and high power, there would be the potential for carbon erosion this could be assessed and corrected for using TDI, or a different coating material could be used.

The measurement of Fe using L-line X-rays allows measurement at low voltage providing high spatial resolution (< 350 nm depth at 7 kV for ulvospinel, Fig. 1) for all the X-rays which can be excited. The results show in keeping with previous findings (e.g., [7, 28]) that the L ℓ -line provides reasonable results (accuracy within ≤ 10 % relative), a substantial improvement from conventional L α -line measurements. The L ℓ measurements clearly require careful selection of the standard, with this having a significant effect on accuracy, and have large errors at low intensities due to the weak intensity of this line. The intensity of the L ℓ -line relative to L α varies with element, becoming more favourable as the atomic number is reduced towards Ti and the occupancy of the 3d shell declines reducing L3-M5 transitions [30, 35]. The results show that whilst conventional L α measurements are highly inaccurate (with discrepancies up to 45 % relative) the use of a calibration curve to calculate Fe concentration can yield good results with accuracy approximating ≤ 5 % for a range of minerals (excluding Fe metal, pyrite and ilmenite) and rendered insensitive to Fe oxidation state when a fixed position is used. Whilst this accuracy is less than achieved in standard high voltage analysis (typically 1 - 2 % relative) and is less robust than the low overvoltage measurements made using the Fe-K α X-ray line, it is a significant result, comparable to measurements made of olivine where the solid-solution MACs and partial fluorescence yields were determined [25]. In this case, inaccuracies of ≤ 4 % were obtained. The main advantage of this approach is the ability to measure olivines, pyroxenes, garnets, and some oxide minerals of varying oxidation state. Simple solid-solution MACs would be unable to account for the variations in MAC with Fe valence changes. If we consider the lateral resolution for this method, again the above measurements were made at 10 μ m beam with a wide spacing to avoid the possibility of carbon erosion and overlapping carbon contamination. At 200 nA and 7 kV the spot size would exceed 150 nm [3], making the lateral resolution worse than the depth resolution. At 7 kV carbon coat erosion would be expected to be worse [14], although the effect on X-ray intensities may be similar or less given the larger overvoltages. Again TDI or other coating materials could be considered. Improvements to the Fe-L depth

resolution could be made by dropping the accelerating voltage, but below 4.97 kV Ti-K cannot be excited, and with reduction in voltage there is an associated increase in spot size, particularly at high beam currents [3].

In the above cases, high beam currents (100 nA - 200 nA) are used to provide high precision. To achieve higher lateral resolution by reducing spot sizes lower beam currents could be used. For Fe K α at low overvoltage the higher intensities would permit a reduction in beam current whilst still maintaining reasonable precision (e.g., 1.6 % relative 2σ for St John's Island olivine with 7.5 wt% Fe at 25nA using 2 spectrometers), although trace element sensitivity would be reduced. In the case of L α X-rays and even more so L ℓ X-rays the lower X-ray intensities using a TAP crystal limit the reduction in beam current whilst maintaining reasonable precision. The samples examined are all stable under the electron beam, whilst this is true of olivine, pyroxene, garnet and spinel it is not true of all minerals notably carbonates and phosphates or glass. In the case of plagioclase the resolution achievable is significantly affected by the stability of the sample requiring a defocussed beam. Saunders *et al.* [36] found that whilst a spatial resolution of ≤ 350 nm could be achieved for orthopyroxene with a 30 nm beam at 5 kV, plagioclase required a 500 nm defocused beam yielding a spatial resolution of ca. 750 nm

7. CONCLUSIONS

The optimum analytical conditions for a given analysis are complex to determine and the maximum spatial resolution achievable is dependable on the elements and material analysed. Low overvoltage and low voltage provide two mechanisms of achieving high resolution, with the resolution a function of the electron range, the spot size and the overvoltage and absorption of a particular element (e.g., [3, 4]). The spot size depends on the precision and sensitivity required, together with the intensity of an X-ray line on a particular diffraction crystal. Maximum spatial resolution will be achieved for major element analysis of X-ray lines > 1 keV, where low beam currents can be used in combination with low overvoltage or low voltage settings, for dense materials (e.g., [1]).

The measurements made demonstrate that low overvoltage measurements can give robust results, regardless of the material being analysed, but are limited to one or a few elements at a given voltage. In addition, low overvoltage is very sensitive to carbon erosion and contamination, which are pronounced at high current density small spot analysis, and tightly spaced analyses respectively. Mitigation methods include TDI correction and other coating materials for carbon erosion [14] and the use of an anticontamination cold-finger and empirical corrections for contamination [17]. Depending on the sample, the use of an oxygen air-jet, stage heating, chamber plasma cleaning or sample preparation using FIB milling or argon cross section polishing may be suitable to reduce contamination [17-21].

Low voltages provide high spatial resolution for all the X-rays excited, equal or less than the interaction volume. It does however restrict the X-rays which can be used. The L-line X-rays of transition metals are particularly problematic. The Fe-La measurements show that despite anomalous absorption and partial fluorescence yields (see [24]) reasonable results ($\leq 5\%$ relative accuracy for a limited range of materials) can be made using either calibration curve, or experimentally determined solid-solution MACs and partial fluorescence yields [25]. The calibration curve at a fixed peak position provides a method of measurement removing sensitivity to Fe valence. A consequence of using the TAP crystal for L-line measurements is the low intensity, requiring high beam currents for high precision particularly at low concentrations, thereby limiting the lateral resolution through larger spot sizes. The choice of low overvoltage or L-line method will therefore depend on the precision and accuracy required and the material analysed, with L-lines requiring a range of standards for calibration curves, or pre calculated solid solution MACs and partial fluorescence yields.

8. ACKNOWLEDGMENTS

We would like to thank the Smithsonian Institute for supplying the Rockport, Fayalite standard (NMNH 85276).

9. REFERENCES

- [1] Kimura T, Nishida K and Tanuma S 2006 *Microchim. Acta* **155** 175-178
- [2] Hovington P, Drouin D and Gauvin R 1997 *Scanning* **19** 1-14
- [3] Pinard P T and Richter S 2014 *IOP Conf. Ser.: Mater. Sci. Engng.* **55** 012016
- [4] McSwiggen P 2014 *IOP Conf. Ser.: Mater. Sci. Engng.* **55** 012009
- [5] Llovet X and Salvat F 2016 *IOP Conf. Ser.: Mater. Sci. Engng.* **109** 012009
- [6] Ritchie N W 2009 *Microsc. Microanal.* **15** 454-468
- [7] Statham P and Holland J 2014 *IOP Conf. Ser.: Mater. Sci. Engng.* **55** 012017
- [8] Kubo Y, Hamada K and Urano A 2003 *Ultramicroscopy* **135** 64-70
- [9] Bastin G F and Heijigers H J M 1990 *Scanning* **12** 225-236
- [10] Chopra D 1970 *Phys. Rev. A* **1** 230-235
- [11] Fischer D W and Baun W L 1967 *J Appl. Phys.* **38** 4830-4836
- [12] Lábár J L and Salter C 1991 in: *Electron probe quantitation.* (Heinrich K F J and Newbury D E; Eds.). (New York, NY: Plenum Press) 223
- [13] Matthews M B, Kearns S L and Buse B 2018 *Microsc. Microanal.* **24** 83-92
- [14] Matthews M B, Kearns S L and Buse B 2018 *Microsc. Microanal.* **24** 612-622
- [15] Matthews M B, Kearns S L and Buse B 2019 *Microsc. Microanal.*, submitted
- [16] Pinard P T, Schwedt A, Ramazani A, Prahl U and Richter S 2013 *Microsc. Microanal.* **19** 996-1006
- [17] Buse B and Kearns S 2015 *Microsc. Microanal.* **21** 594-605

- [18] Bastin G F and Heijligers H J M 1988 in: *Microbeam analysis.* (Newbury D E; Ed.). (San Francisco, CA: San Francisco Press) 325
- [19] Buse B, Kearns S, Clapham C and Hawley D 2016 *Microsc. Microanal.* **22** 981-986
- [20] Augustyn E, Hallstedt B, Wietbrock B, Mayer J, Schwedt A and Richter S 2012 *IOP Conf. Ser.: Mater. Sci. Engng.* **32** 012001
- [21] Yamashita T, Tanaka Y, Yagoshi M and Ishida K 2016 *Sci. Rep-UK* **6** 29825
- [22] Pouchou J L and Pichoir F 1985 *J. Microsc. Spectrosc. Electron.* **10** 291-294
- [23] Fialin M 1990 *X-ray Spectrom.* **19** 169-172
- [24] Llovet X, Pinard P T, Heikinheimo E and Louhenkilpi S 2016 *Microsc. Microanal.* **22** 1233-1243
- [25] Buse B and Kearns S L 2018 *Microsc. Microanal.* **24** 1-7
- [26] Moy A and Fournelle J 2018 *Microsc. Microanal.* **24** (Suppl. 1)
- [27] Rémond G, Myklebust R, Fialin M, Nockolds C, Phillips M and Roques-Carnes C 2002 *J. Res. Natl. Inst. Stand. Technol.* **107** 509-529
- [28] Gopon P, Fournelle J, Sobol P E and Llovet X 2013 *Microsc. Microanal.* **19** 1698-1708
- [29] Buse B and Kearns S L 2011 in: *Book of Abstracts of the European Microbeam Analysis Society 12th European Workshop.* (Angers, France; 15-19 May)
- [30] Wyckoff R W G and Davidson F D 1965 *J. Appl. Phys.* **36** 1883-1885
- [31] Okada M 1981 *J. Radioanal. Chem.* **63** 201-204
- [32] Fialin M, Wagner C, Métrich N, Humler E, Galois L and Bézou A 2001 *Amer. Mineralogist* **86** 456-465
- [33] Hofer H E and Brey G P 2007 *Amer. Mineralogist* **92** 873-885
- [34] Moy A and Fournelle J 2017 *Microsc. Microanal.* **23** (Suppl. 1)
- [35] Holliday J E 1962 *J. Appl. Phys.* **33** 3259-3265
- [36] Saunders K, Buse B, Kilburn M R, Kearns S and Blundy J 2014 *Chem. Geol.* **364** 20-32